



Liu, X., Azarpeyvand, M., & Joseph, P. (2015). On the acoustic and aerodynamic performance of serrated airfoils. Paper presented at The 22nd International Congress on Sound and Vibration, Florence, France.

Publisher's PDF, also known as Version of record

[Link to publication record in Explore Bristol Research](#)
PDF-document

University of Bristol - Explore Bristol Research

General rights

This document is made available in accordance with publisher policies. Please cite only the published version using the reference above. Full terms of use are available:
<http://www.bristol.ac.uk/pure/about/ebr-terms.html>



ON THE AERODYNAMIC PERFORMANCE OF SERRATED AIRFOILS

Xiao Liu, Mahdi Azarpeyvand and Raf Theunissen

University of Bristol, Bristol, BS8 1TR, United Kingdom

This paper is concerned with the aerodynamic and aeroacoustic performance of airfoils with serrated trailing- or leading-edges. A great deal of research has been directed toward the application of different types of serrations for the control of airfoil trailing- and leading-edge noise. Prior research has shown that such passive treatments are capable of reducing the airfoil noise over a wide range of frequencies. However, the aerodynamic performance of such treated airfoils has received very little research attention. To better understand the effects of serrations, the aerodynamic performance of serrated airfoils has been studied experimentally. A symmetric NACA 0012 and an asymmetric NACA 65(12)-10 airfoil have been chosen for this study and different serrations have been tested on the leading or trailing-edge. The steady aerodynamic forces, *i.e.* lift and drag, have been measured over a wide range of wind speeds and angles of attack. Preliminary results have shown that despite the noise reduction capability of such passive treatments, they can also significantly change the aerodynamic behavior of the airfoil.

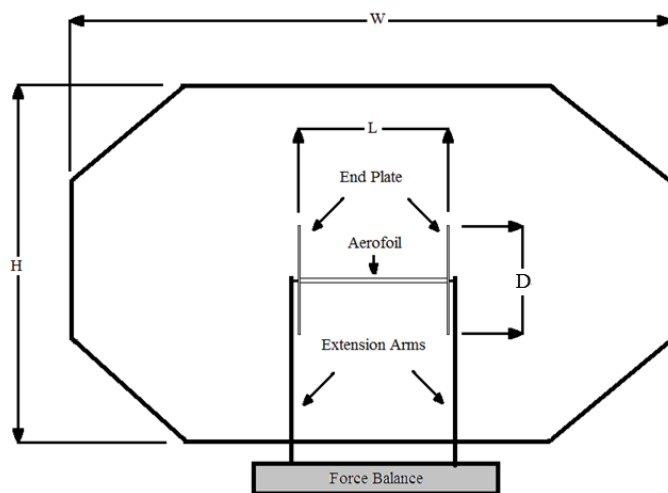
1. Introduction

The use of passive flow control methods for reducing airfoil noise has been the subject of much research. In particular, trailing- and leading-edge serrations have received the greatest attention [1-11]. It has been shown analytically [1, 2] and experimentally [3-9] that the use of trailing- and leading-edge serrations can lead to significant noise reduction over a wide range of frequencies. In a recent study, Gruber *et al.* [5] experimentally studied airfoil trailing-edge noise reduction by applying different types of trailing-edge serrations, namely, sawtooth, slotted-sawtooth and random profiles. It was shown that by optimizing the trailing-edge serration geometry, one can significantly reduce the scattering efficiency at the trailing-edge. Results had shown that the broadband noise reductions of up to 5dB can be obtained using the slotted-sawtooth over a wide frequency range. In the case of turbulence interaction noise, it has been shown that leading-edge serrations can effectively reduce the radiated noise [8-11]. Although the aeroacoustic performance of trailing- and leading-edges has been studied extensively in recent years, no proper study has been carried on the aerodynamic performance of such passive treatments. In this paper, we shall focus on the aerodynamic performance of serrated airfoils, *i.e.* serrated trailing- and leading-edges. Aerodynamic lift and drag measurements will be carried out for symmetric and asymmetric airfoils over a wide range of Reynolds number and angles of attack.

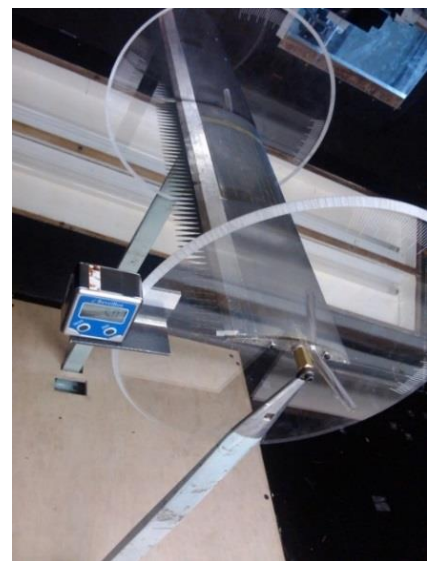
2. Experimental setup

2.1 Aerodynamic force measurement

The aerodynamic force measurements have been carried out in the University of Bristol's 5'x7' closed return wind tunnel with an octagonal working section of 2.1m (wide) and 1.5m (high) with a stable velocity range of 10 m/s to 60 m/s. A schematic of the wind tunnel test section, airfoil and the force balance system is provided in Figure 1. The airfoil and circular endplates (with diameter of $D = 34$ cm) are fixed on the force balance extension arms, see Fig. 1-b. An AMTI OR6-7-2000 force balance was used in this project. The voltage induced from the force balance passes through an AMTI MSA-6 strain gauge amplifier and is converted into data using a control system built in LabVIEW system design software. After carrying out a data quality analysis, sampling frequency of 37 Hz was found to give the best data independency and least uncertainty. Data has been collected for three sets of 10 seconds.



(a)



(b)

Figure 1. Wind tunnel setup for force measurements. (a) Cross-section sketch of wind tunnel setup. (b) Photo of a serrated airfoil in the wind tunnel.

2.2 Models

In order to carry out a comprehensive study, the aerodynamic performance for two airfoils has been investigated, namely, a symmetrical NACA 0012 and an asymmetrical cambered NACA 65(12)-10 airfoil. The airfoils have an effective chord length of $c = 0.155$ m and span length of $L = 0.45$ m, see Figs 2-4.

Airfoils with Serrated Trailing-edge

The test airfoils shown in Figure 2 are composed of a main body (0.14m in chord; made of Green Prolab composite material) and a serration insert. As shown in Fig. 2, 10mm of the trailing-edge part of the airfoils has been cut with a 15mm deep and 0.8 mm thick slot through the edge and along the span in order to allow flat plate serration inserts to be fitted to the airfoil.

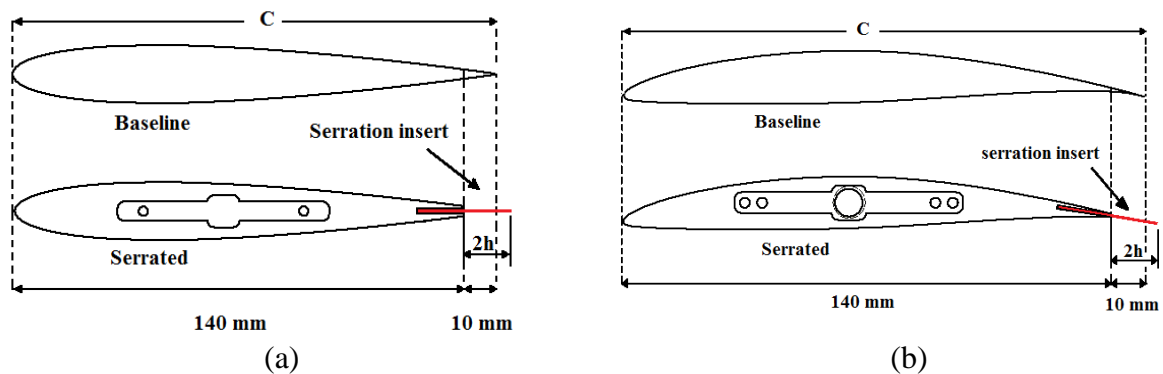


Figure 2. Trailing-edge treatment models (a) Drawings of untreated (baseline) and serrated NACA 0012. (b) Drawings of untreated (baseline) and serrated NACA 65(12)-10.

Based on the analytical and experimental results for noise reduction using trailing-edge serrations [1-5], three types of serrations with good noise reduction performance have been selected for this study. These three types of serrations are sawtooth serrations, sinusoidal serrations and slotted-sawtooth serrations. As shown in Figure 3 and Table 1, nine serrations with different geometrical parameters (amplitude $2h$, periodicity wavelength λ , angle of serration edge α_s , slot width d and slot depth H) have been used for aerodynamic performance measurements.

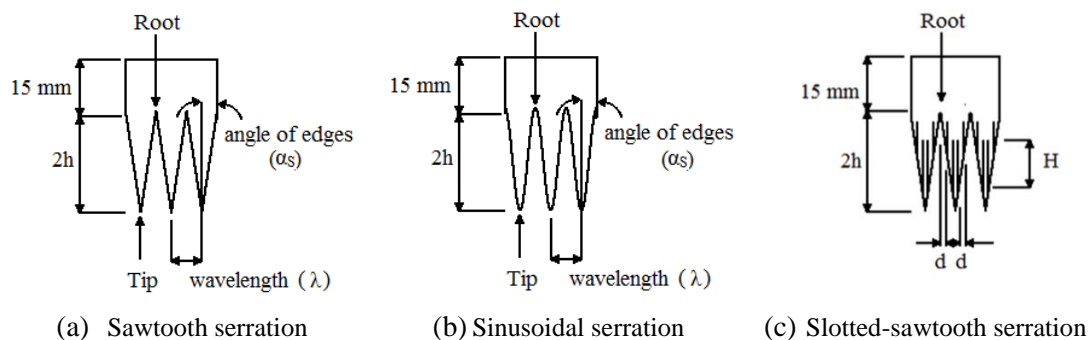


Figure 3. Schematic of different trailing-edge serrations

Table 1 Geometrical parameters of trailing-edge serrations

| Cases | Serration types | $2h$ | λ | λ/h | α_s | d | H |
|--------|-----------------------------------|------|-----------|-------------|------------|-----|-----|
| | | mm | mm | | degrees | mm | mm |
| Case 1 | Baseline (straight trailing-edge) | 15 | - | - | - | - | - |
| Case 2 | Baseline (straight trailing-edge) | 0 | - | - | - | - | - |
| Case 3 | sawtooth | 30 | 3 | 0.2 | 2.86 | - | - |
| Case 4 | sawtooth | 30 | 9 | 0.6 | 8.53 | - | - |
| Case 5 | sawtooth | 30 | 22.5 | 1.5 | 45 | - | - |
| Case 6 | slotted-sawtooth | 30 | 9 | 0.6 | 8.53 | 0.5 | 15 |
| Case 7 | slotted-sawtooth | 30 | 9 | 0.6 | 8.53 | 0.5 | 5 |
| Case 8 | sinusoidal | 30 | 9 | 0.6 | 8.53 | - | - |
| Case 9 | sinusoidal | 30 | 22.5 | 1.5 | 45 | - | - |

Airfoils with Serrated Leading-edge

The effect of leading-edge serrations on the control of turbulence-leading-edge interaction noise has been the subject of much research [8-11]. Here, we have considered the aerodynamic performance

of airfoils with different leading-edge serrations. Eight airfoils based on NACA 0012 and NACA 65(12)-10 geometries, with chord length of 0.15m, with different leading-edge profiles have been designed and made using CNC machining. Figure 4 (a) shows the top view of the models and cross-section view of the tip and root positions of the sawtooth leading-edge models. As shown in Figure 4 (b) and (c), the geometry modification only affects the leading-edge region of the airfoil and the rest of the airfoil remains unchanged. The geometrical details of the airfoils used in this study are provided in Table 2.

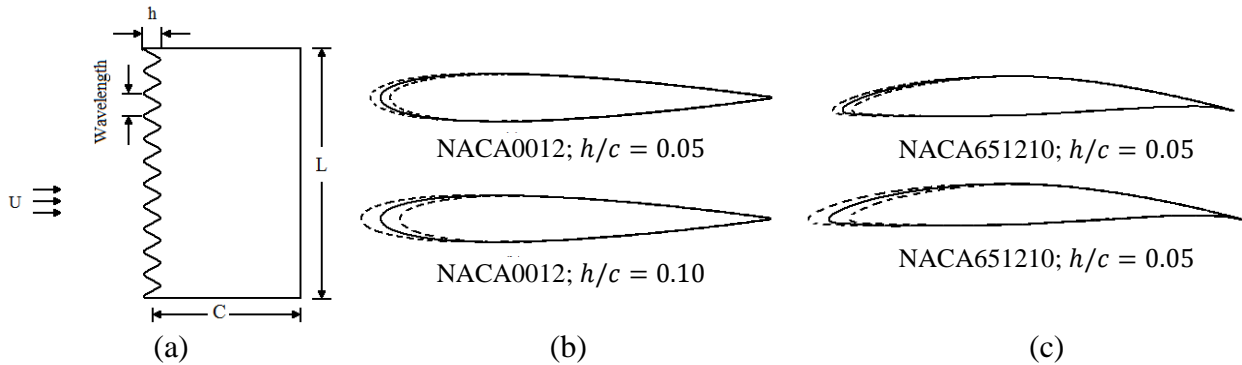


Figure 4. Drawings of leading-edge serration models. (a) Top view of an airfoil with leading-edge serration. (b) Cross section view of NACA 0012 airfoil with leading-edge serration, (c) Cross section view of NACA 65(12)-10 airfoil with leading-edge serration.

Table 2. Geometrical parameters of leading-edge serrations

| | Airfoil | h/c | λ/c |
|----------|----------------|-------|-------------|
| Model 1 | NACA 0012 | 0 | 0 |
| Model 2 | NACA 0012 | 5% | 6% |
| Model 3 | NACA 0012 | 10% | 6% |
| Model 4 | NACA 0012 | 5% | 15% |
| Model 5 | NACA 0012 | 10% | 15% |
| Model 6 | NACA 65(12)-10 | 0 | 0 |
| Model 7 | NACA 65(12)-10 | 5% | 6% |
| Model 8 | NACA 65(12)-10 | 10% | 6% |
| Model 9 | NACA 65(12)-10 | 5% | 15% |
| Model 10 | NACA 65(12)-10 | 10% | 15% |

3. Results and Discussion

In this section, we shall provide results for lift and drag of NACA 0012 and NACA 65(12)-10 airfoils with trailing- and leading-edge serrations. Wind tunnel experiments have been carried out over a wide range of flow speeds, $U = 20 \text{ m/s}$ to 60 m/s . The NACA 0012 and NACA 65(12)-10 airfoils have been tested over an angle of attack (AoA) range of 0° to 20° and -5° to 20° , respectively, covering small AoAs (relevant to prior research on trailing- and leading edge noise [3-5, 8-11]) and stall regions.

3.1 Airfoils with trailing-edge serration

Figures 5 through 7 present the results of lift and drag coefficients for a NACA 65(12)-10 airfoil with and without (baseline) trailing-edge serration, over angle of attack range of -5° to 20° . Wind tunnel tests have been carried out between 20 m/s to 60 m/s , but we only present the results for 30 m/s , and 50 m/s here. Figure 5 presents the lift and drag results for three sawtooth serrations with wavelengths of $\lambda = 3 \text{ mm}$, 9 mm and 22 mm and amplitude of $2h = 30 \text{ mm}$. Results have also been compared with 155 mm chord (effective chord length) and 140 mm chord baselines (no trailing-edge insert, see Fig. 2).

The results of sawtooth serrations have shown that for all wind speeds considered in this study, the lift coefficient of the airfoils fitted with $\lambda = 9 \text{ mm}$ and 22.5 mm serrations reduces up to 15% compared with the 150mm chord baseline over the AoA range of -5° to about 10° . Results have also shown that the trailing-edge serrations increase the lift coefficient in the pre-stall region but do not particularly change the stall behavior ($C_L - \alpha$ curves) of the airfoil. Furthermore, it has been observed that serrations do not significantly change the drag coefficient of the airfoil between AoAs of -5° to 10° . For angles of attack larger than 10° , the drag coefficient of serrated trailing-edge is generally higher than the baseline and it can also be seen that serrations with large wavelengths produce more drag. The results for sinusoidal serrations, Fig. 6, show very similar trends to that of sawtooth serration (Fig. 5). The lift and drag results for a NACA 65(12)-10 airfoil fitted with slotted-sawtooth serrations are presented in Fig. 7. The base sawtooth has a wavelength of $\lambda = 9 \text{ mm}$ and amplitude of $2h = 30 \text{ mm}$ and has slot cuts of $H = 5 \text{ mm}$ and 15 mm (see Fig. 3-c). Results have shown that the use of slotted-sawtooth serrations can result in up to 30% reduction in the lift coefficient over the entire AoA range. The maximum reduction has been observed at small angle of attack region. It is worth mentioning here that based on analytical and experimental results in [1-5], sharp sawtooth (small α_s) and slotted-sawtooth serrations are expected to provide large and robust noise reduction over a wide frequency range. The aerodynamic results, however, have revealed that such treated airfoils (effective in term of noise) can also be prone to aerodynamic losses.

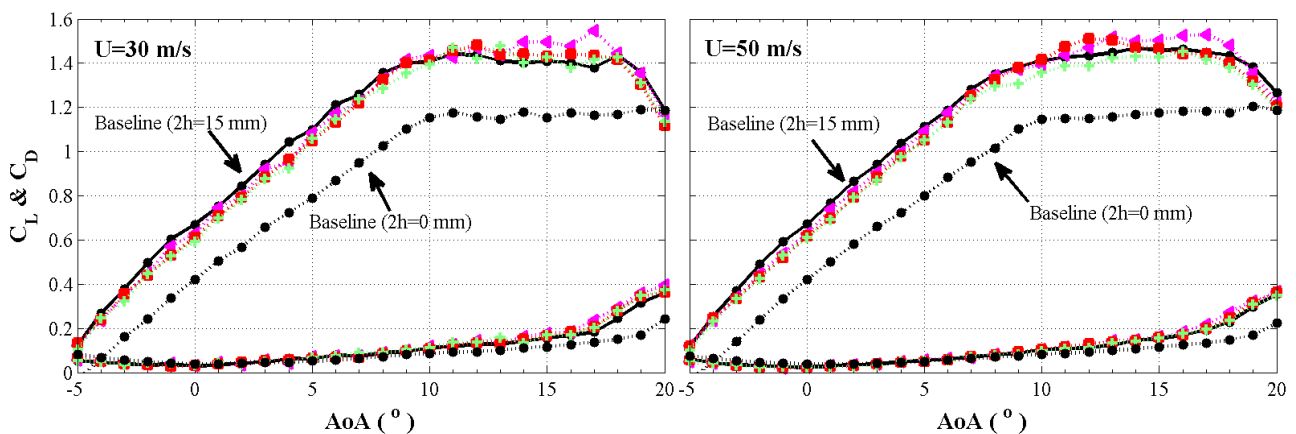


Figure 5. Lift and drag coefficients for a NACA 65(12)-10 airfoil fitted with different sawtooth serrations ($2h = 30 \text{ mm}$). Triangles: $\lambda = 22.5 \text{ mm}$; squares: $\lambda = 9 \text{ mm}$; pluses: $\lambda = 3 \text{ mm}$.

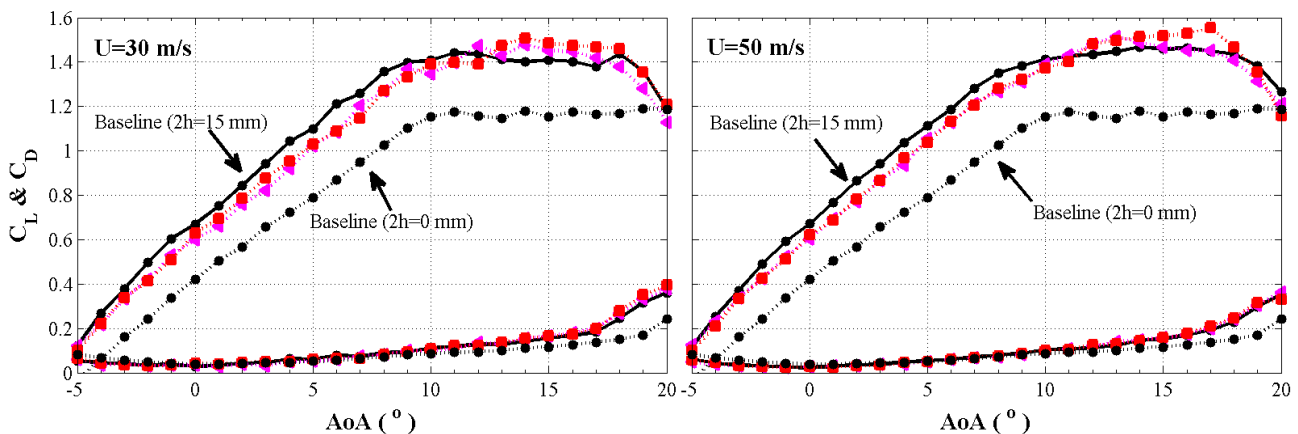


Figure 6. Lift and drag coefficients for a NACA 65(12)-10 airfoil fitted with different sinusoidal serrations ($2h = 30 \text{ mm}$). Triangles: $\lambda = 22.5 \text{ mm}$; squares: $\lambda = 9 \text{ mm}$.

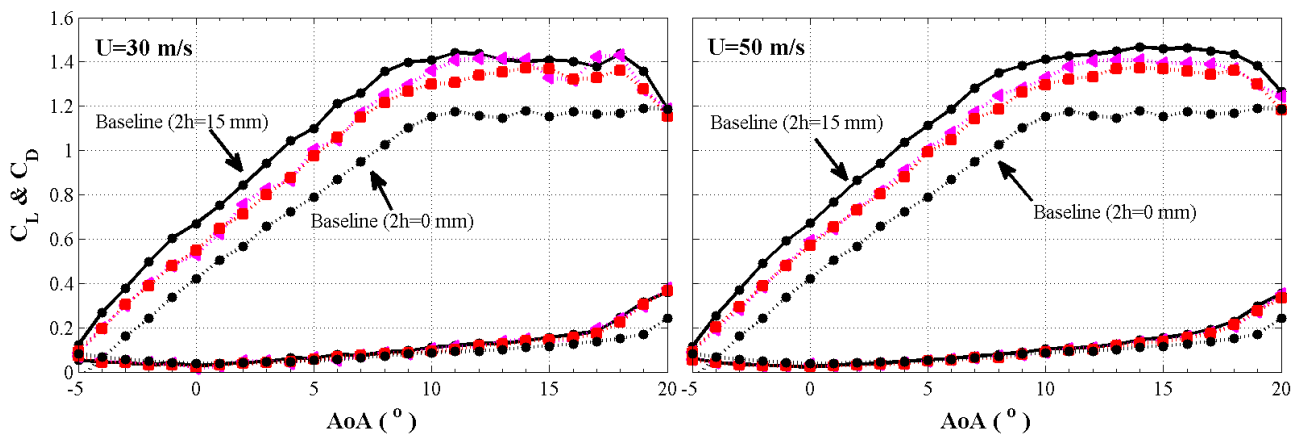


Figure 7. Lift and drag coefficients for a NACA 65(12)-10 airfoil fitted with different slotted-sawtooth serrations ($\lambda = 9 \text{ mm}$, $2h = 30 \text{ mm}$, $d = 0.5 \text{ mm}$). Triangles: $H = 5 \text{ mm}$; squares: $H = 15 \text{ mm}$.

Figure 8 presents the results of lift and drag coefficients of a NACA 0012 fitted with different sawtooth serrations ($\lambda = 3 \text{ mm}$ and 9 mm ; amplitude of $2h = 30 \text{ mm}$) and slotted sawtooth serrations ($\lambda = 9 \text{ mm}$, $2h = 30 \text{ mm}$, $d = 0.5 \text{ mm}$ $H = 5 \text{ mm}$ and 15 mm), at wind speeds of 30 m/s and 50 m/s over the angle of attack range of 0° to 20° . The lift coefficient results for NACA0012 at small AoAs is very different from those observed in Figs. 5-7 for NACA 65(12)-10. The effect of serration on the lift coefficient is less significant than those observed for NACA 65(12)-10, particularly at low speeds. Over the critical AoA region, 12° to 15° , serrations can lead to significant reduction of the maximum lift coefficient ($C_{L,max}$), but can also improve the lift performance in deep stall region (17° to 20°). It has also been observed that the drag of NACA 0012 airfoils fitted with serrations is generally lower than the NACA 00112 with straight trailing edge (155 mm chord).

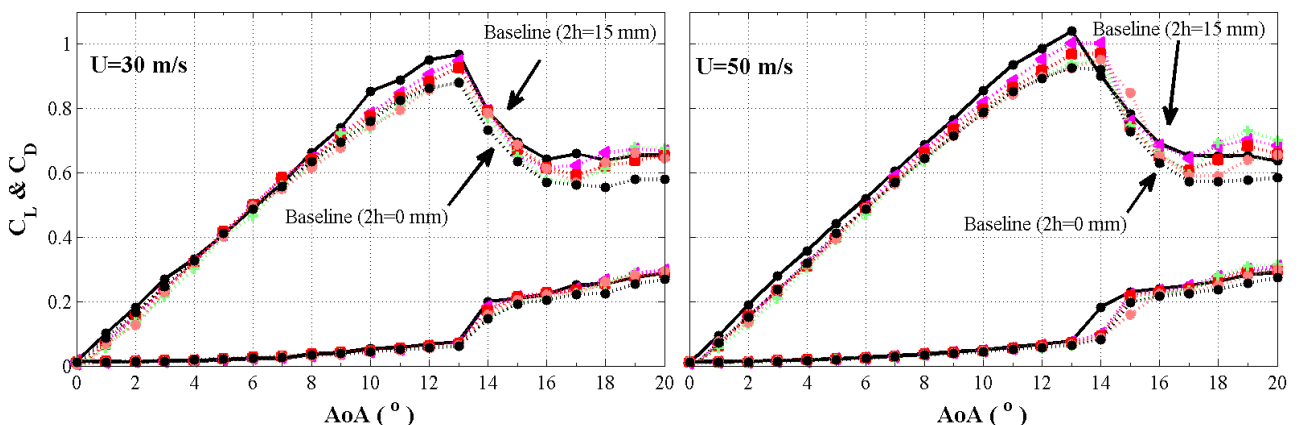


Figure 8. Lift and drag coefficients for a NACA 0012 airfoil fitted with different serrations ($2h = 30 \text{ mm}$). Triangles: $\lambda = 9 \text{ mm}$; squares: sawtooth serration with $\lambda = 3 \text{ mm}$ wavelength; pluses: slotted-sawtooth serration with $\lambda = 9 \text{ mm}$, $d = 0.5 \text{ mm}$ and $H = 5 \text{ mm}$; stars: slotted-sawtooth serration with $\lambda = 9 \text{ mm}$, $d = 0.5 \text{ mm}$ and $H = 15 \text{ mm}$.

3.2 Airfoils with leading-edge serration

Figure 9 presents the results of lift and drag coefficients for a NACA 65(12)-10 airfoil with leading-edge serrations (Table 2) over the AoA range of -5° to 20° , and wind speeds of 30 m/s , and

50m/s. Results are presented for serrations with different wavelengths (0.05c and 0.15c) and amplitudes (0.06c and 0.10c), as listed in Table 2. The lift coefficient results for all four serration cases show a significant reduction, up to 40% in the pre-stall region. Results have also shown that the leading-edge serrations significantly change the stall behavior of the airfoil. An untreated NACA 65(12)-10 (baseline) has an almost constant lift coefficient over 8° to 19°, while serrated NACA 65(12)-10 airfoils experience a sharp stall in the AoA range of 12° to 15°, depending on the serration type. Results have also shown that leading-edge serrations can significantly reduce the drag coefficient at low AoAs. Figure 10 presents the aerodynamic performance of serrated and unserrated NACA 0012 airfoils over the AoA range of 0° to 20°. The effect of leading-edge serrations for NACA0012 is very different from that of NACA 65(12)-10. Results have shown slight improvement in the lift coefficient of serrated NACA 0012 airfoils over 0° to 8°. The sharp stall behavior of NACA 0012 also changes significantly, leading to a flat C_L over AoA range of 10° to 17°. It is evident from Fig. 9 and 10 that leading-edge serrations can significantly reduce the maximum lift ($C_{L,max}$) and lift-to-drag ratio (C_L/C_D) over the stall region. Results have also shown that in the case of NACA 0012 the use of leading-edge serrations does not have a noticeable effect on the drag coefficient at small AoAs, but it generally increases C_D near the stall region (10° to 15°).

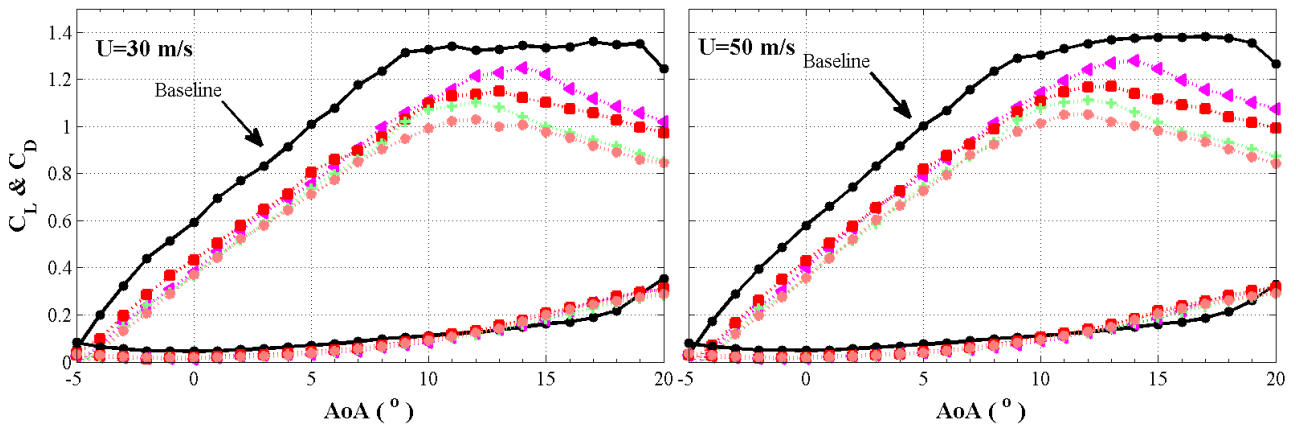


Figure 9. Lift and drag coefficients for a NACA 65(12)-10 airfoil with leading-edge serration. Triangles: $\lambda/c = 0.15$ and $h/c = 0.05$; squares: $\lambda/c = 0.15$ and $h/c = 0.10$; pluses: $\lambda/c = 0.06$ and $h/c = 0.05$; stars: $\lambda/c = 0.06$ and $h/c = 0.10$.

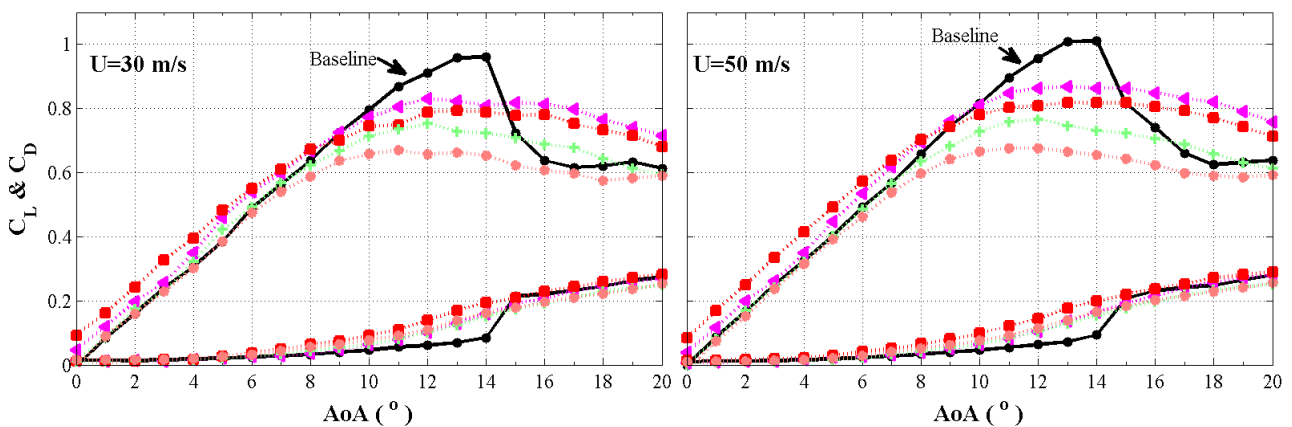


Figure 10. Lift and drag coefficients for a NACA 0012 airfoil with leading-edge serration. Triangles: $\lambda/c = 0.15$ and $h/c = 0.05$; squares: $\lambda/c = 0.15$ and $h/c = 0.10$; pluses: $\lambda/c = 0.06$ and $h/c = 0.05$; star marker: $\lambda/c = 0.06$ and $h/c = 0.10$.

4. Conclusions

The aerodynamic performance of airfoils with leading and trailing-edge serrations has been studied. Prior studies had shown that such treatments can significantly reduce the noise from airfoils. However, the results in this paper show that the trailing- and leading-edge serrations can also significantly change the aerodynamic performance of the airfoil. It has also been shown that the level of the changes depends greatly on the type of the airfoil as well as the geometrical details of the serrations. In the case of trailing-edge serrations it has been observed that serrations can significantly reduce the aerodynamic lift of airfoils but the overall shape of $C_L - \alpha$ curves and the stall properties of the airfoil do not change considerably. Leading-edge serrations, on the other hand, can alter the shape of $C_L - \alpha$ curves and the stall properties of the airfoil, besides its lift and drag performance. From the results presented above, it is evident that more in depth studies are needed if trailing- and leading-edge treatments are to be used as a solution for airfoil noise.

REFERENCES

- 1 Howe, M. S., Noise produced by a sawtooth trailing-edge. *Journal of the Acoustical Society of America*, **90**(1), 482–487, (1991).
- 2 Azarpeyvand, M., Gruber, M., Joseph, P. F., An Analytical Investigation of Trailing-edge Noise Reduction Using Novel Serrations, *19th AIAA/CEAS Aeroacoustics Conference*, May (2013).
- 3 Gruber, M., Joseph, P. F. and Azarpeyvand, M., An experimental investigation of novel trailing-edge geometries on aerofoil trailing-edge noise reduction, *19th AIAA/CEAS Aeroacoustics Conference*, May (2013).
- 4 Gruber, M., Azarpeyvand, M., and Joseph, P. F., Airfoil trailing-edge noise reduction by the introduction of sawtooth and slitted trailing-edge geometries, *20th International Congress on Acoustics*, Sydney, Australia, 23 – 27, August (2010).
- 5 Gruber, M., *Aerofoil noise reduction by edge treatments*, Doctoral Thesis, University of Southampton, Faculty of Engineering and the Environment, (2012).
- 6 Oerlemans, S., Fisher, M., Maeder, T. and Kögler, K., Reduction of wind turbine noise using optimized aerofoils and trailing-edge serrations. *AIAA journal*, **47**, 1470 – 1481, (2009).
- 7 Moreau, D. J., and Con J. D., Noise-reduction mechanism of a flat-plate serrated trailing-edge. *AIAA journal*, **51**(10), 2513– 2522, (2013).
- 8 Soderman, P. T., Leading-edge serrations which reduce the noise of low-speed rotors, NASA technical note, NASA TN D-7371, (1973).
- 9 Hersh, A. S., Soderman, P. T. and Hayden, R. E., Investigation of acoustic effects of leading-edge serrations on airfoils, *Journal of aircraft American Institute of Aeronautics and Astronautics*, **11**(4), 197–202 (1974).
- 10 Lau, A. S. H., Haeri, S. and Kim, J. W., The effect of wavy leading-edges on aerofoil-gust interaction noise, *Journal of Sound and Vibration*, **332**, 6234–6253, (2013).
- 11 Clair, V., Polacsek, C., Le Garrec, T., Reboul, G., Gruber, M. and Joseph, P. F., Experimental and numerical investigation of turbulence-airfoil noise reduction using wavy edges, *AIAA journal*, **51**(11), 2695–2713, (2013).